

Direct Ink Writing of a Light-Responsive Underwater Liquid Crystal Actuator with Atypical Temperature-Dependent Shape Changes

Citation for published version (APA):

del Pozo Puig, M., Liu, L., Pilz Da Cunha, M., Broer, D. J., & Schenning, A. P. H. J. (2020). Direct Ink Writing of a Light-Responsive Underwater Liquid Crystal Actuator with Atypical Temperature-Dependent Shape Changes. *Advanced Functional Materials*, 30(50), Article 2005560. <https://doi.org/10.1002/adfm.202005560>

Document license:
TAVERNE

DOI:
[10.1002/adfm.202005560](https://doi.org/10.1002/adfm.202005560)

Document status and date:
Published: 08/12/2020

Document Version:
Publisher's PDF, also known as Version of Record (includes final page, issue and volume numbers)

Please check the document version of this publication:

- A submitted manuscript is the version of the article upon submission and before peer-review. There can be important differences between the submitted version and the official published version of record. People interested in the research are advised to contact the author for the final version of the publication, or visit the DOI to the publisher's website.
- The final author version and the galley proof are versions of the publication after peer review.
- The final published version features the final layout of the paper including the volume, issue and page numbers.

[Link to publication](#)

General rights

Copyright and moral rights for the publications made accessible in the public portal are retained by the authors and/or other copyright owners and it is a condition of accessing publications that users recognise and abide by the legal requirements associated with these rights.

- Users may download and print one copy of any publication from the public portal for the purpose of private study or research.
- You may not further distribute the material or use it for any profit-making activity or commercial gain
- You may freely distribute the URL identifying the publication in the public portal.

If the publication is distributed under the terms of Article 25fa of the Dutch Copyright Act, indicated by the "Taverne" license above, please follow below link for the End User Agreement:

www.tue.nl/taverne

Take down policy

If you believe that this document breaches copyright please contact us at:

openaccess@tue.nl

providing details and we will investigate your claim.

Direct Ink Writing of a Light-Responsive Underwater Liquid Crystal Actuator with Atypical Temperature-Dependent Shape Changes

Marc del Pozo, Li Liu, Marina Pilz da Cunha, Dirk J. Broer, and Albert P. H. J. Schenning*

In recent years, light-responsive liquid crystal (LC) polymers have been studied as promising materials for the fabrication of untethered soft actuators. The underwater behavior of these advanced materials has, however, been rarely investigated. This paper reports on the fabrication of light-responsive amphibious LC-actuators via direct ink writing (DIW). The actuators present two underwater deformation modes triggered by different stimuli. Temperature induces contraction/expansion and light induces bending/unbending. Unexpectedly, temperature can regulate the bending directionality, giving the material additional versatility to its deformation modes. These findings serve as a toolbox for the fabrication of light-responsive actuators via DIW that operate in air and underwater.

1. Introduction

Untethered liquid crystalline (LC) actuators are of increasing interest in many applications including microfluidics, biomedical engineering, and soft robotics.^[1] Typically, these actuators respond to external stimuli such as temperature,^[2–5] humidity,^[6,7] light,^[8–11] or magnetic fields.^[12,13] Among them, light is a versatile and promising platform to control the

movement of these actuators in an easy and rapid manner.^[14,15] Light-responsive LC actuators have been previously obtained by introducing azobenzene photoswitches.^[16,17] Although considerable progress has been achieved in photoactuation in air,^[8,9,18–20] there are few examples of LC actuators that are responsive underwater.^[21,22] Additionally, it has been shown that by utilizing humidity, the light response of an LC film can be enabled or disabled.^[19] Furthermore, temperature can enhance the extent of motion^[23] or reverse the directionality of the light-driven bending motion.^[24] These examples demonstrate the potential of combining

different stimuli-responses in a single material to increase the versatility and control of actuation. Thereto, it is interesting to explore and design new LC precursors to obtain light-fueled actuators active underwater and investigate the effect of other stimuli, such as temperature, in their photoactuation.


For the fabrication of soft actuators, additive manufacturing (AM) is an attractive method.^[25] AM has the ability to rapidly fabricate complex 3D objects at different length scales using a variety of materials.^[26] In recent years, the direct ink writing (DIW) of liquid crystal elastomer (LCE) has emerged as a promising approach to fabricate soft actuators displaying distinct deformation modes.^[2,27–35] Until now, most of these LCE-based actuators fabricated via DIW have shown reversible temperature-triggered shape changes, but no example shows light-triggered motion. It would be appealing to develop inks suitable for DIW equipment that can be used to fabricate light-responsive LCE actuators.

Herein, we developed an LC-based ink for the fabrication of temperature- and light-responsive amphibious actuators via DIW. The ink was first tested on fibers drawn from droplets on a glass surface, as this method has some similarities with respect to the DIW process. Photoactuation of the fibers showed an atypical bending away from the light source motion. We determined that the underlying mechanism for this response is a smectic C (Sm C) to smectic A (Sm A) photoinduced phase transition. This same ink was then used to fabricate a light-fueled underwater LCE-based actuator via DIW. The planar aligned film contracted/expanded in response to temperature changes and bent away from the light source when illuminated at room temperature. Interestingly, when the film was photoactuated at ≈ 60 °C in water, it bent toward the light source. This temperature-dependent directionality of the light-triggered bending motion is the result of the different LC phases obtained

M. del Pozo, L. Liu, M. Pilz da Cunha, Prof. D. J. Broer, Prof. A. P. H. J. Schenning
Stimuli-responsive Functional Materials and Devices
Department of Chemical Engineering
Eindhoven University of Technology
P.O. Box 513, Eindhoven 5600 MB, Netherlands
E-mail: a.p.h.j.schenning@tue.nl

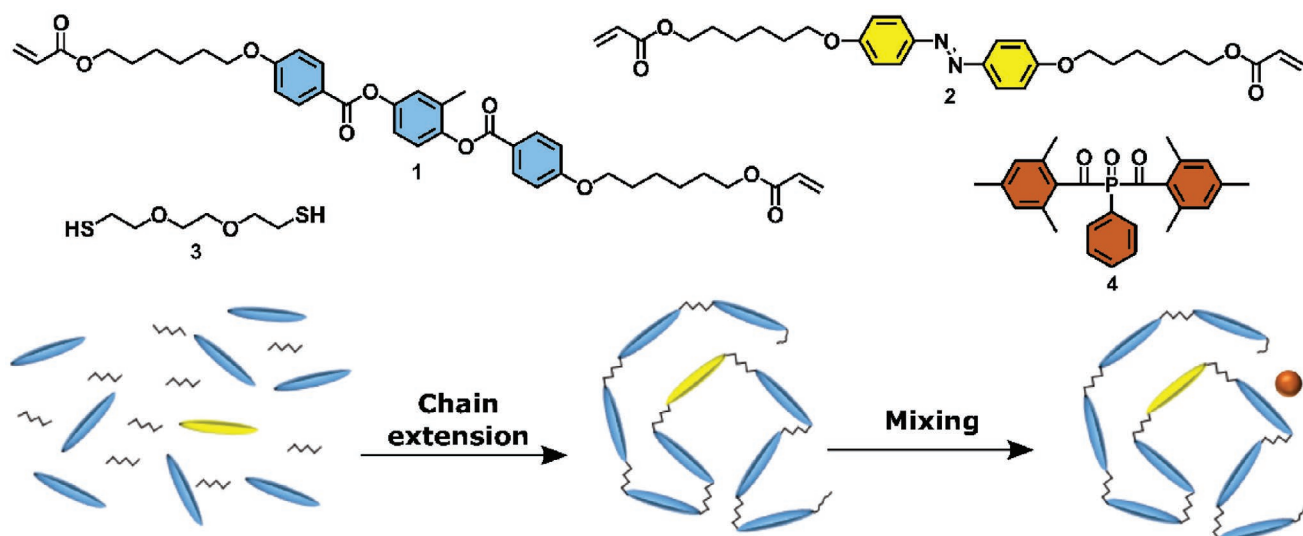
L. Liu
School of Chemistry and Chemical Engineering
Jiangsu Province Hi-Tech Key Laboratory for Bio-Medical Research
State Key Laboratory of Bioelectronics
Institute of Advanced Materials
Southeast University
Nanjing 211189, China

L. Liu, M. Pilz da Cunha, Prof. D. J. Broer, Prof. A. P. H. J. Schenning
Institute for Complex Molecular Systems
Eindhoven University of Technology
Den Dolech 2, Eindhoven 5612 AZ, Netherlands

 The ORCID identification number(s) for the author(s) of this article can be found under <https://doi.org/10.1002/adfm.202005560>.

© 2020 The Authors. Published by Wiley-VCH GmbH. This is an open access article under the terms of the Creative Commons Attribution License, which permits use, distribution and reproduction in any medium, provided the original work is properly cited.

DOI: 10.1002/adfm.202005560



Scheme 1. Preparation of ink and chemical composition used in the ink: the reactive mesogens (blue), azobenzene (yellow), di-thiol spacer (black), and photoinitiator (orange).

at different temperatures. As a result, a temperature-controlled light-induced bending of the film is achieved.

2. Results and Discussion

2.1. Light-Responsive Ink for Direct Ink Writing

An LC-based ink for the fabrication of amphibious light responsive actuators via DIW equipment needs to fulfill two critical parameters: 1) shear thinning to achieve control over the molecular alignment during printing^[31,33] and 2) incorporation of a reactive azobenzene molecule as a crosslinker in order to get a photoresponse underwater,^[22] preferably in the main chain oligomer since this enhances the extent of the photoactuation.^[36] Taking these requirements into account, we modified an already reported ink for fiber drawing^[23] by incorporating the azobenzene into the main chain LC oligomer (**Scheme 1**). The chemical composition for the oligomer consists of reactive mesogens 1,4-bis-[4-(6-acryloyloxyhexyloxy) benzoyloxy]-2-methylbenzene (**1**), photoresponsive moiety 4,4'-bis(6-acryloyloxyhexyloxy) azobenzene (**2**), and isotropic chain extender 3,6-dioxa-1,8-octanedithiol (**3**). The acrylate-terminated main chain LC oligomer was synthesized via a base-catalyzed thiol-Michael addition reaction with a slight excess of acrylate versus thiol. After chain extension, the ¹H-NMR spectrum shows signals between 6.40–5.70 ppm (Figure S1, Supporting Information), implying the presence of acrylate end groups. As evidenced in the gel permeation chromatography (GPC) spectrum (Figure S2, Supporting Information), the characteristic absorption of *trans*-azobenzene peak at ≈ 365 nm and the absorption of the other moieties at ≈ 250 nm are at the same retention time, revealing that azobenzene molecules were indeed incorporated into the main chain oligomer. Based on GPC data, the weight average molecular weight was evaluated as $\approx 18\,000$ g mol⁻¹. Differential scanning calorimetry (DSC) traces and crossed polarized microscopy

showed a smectic to nematic phase transition temperature ($T_{Sm/N}$) at ≈ 49 °C and a nematic to isotropic phase transition temperature ($T_{N/I}$) at 81 °C (Figure S3, Supporting Information).

Characterization of the photoactuation of the resulting LCE network was first performed by drawing fibers standing on a glass substrate using a previous reported procedure.^[23] This fiber drawing method has many similarities with DIW (vide infra) with respect to precursor rheology, polymer properties after UV curing, and response to light for actuation. The fibers had a diameter of ≈ 120 μ m and a length of ≈ 9 mm. DSC traces of the fiber revealed a glass transition temperature (T_g) at approximately -16 °C and a broad $T_{N/I}$ centered at 74 °C (Figure S4, Supporting Information). The photoactuation of the fibers was investigated in air, at room temperature, and under the illumination of both UV (365 nm, 75 mW cm⁻²) and visible (455 nm, 30 mW cm⁻²) lights. Unexpectedly, when exposed to UV light, the fibers bent away from the light source (**Figure 1**; **Movie S1**, Supporting Information). A maximum bending angle of approximately -62° was achieved within 60 s of UV irradiation (Figure 1). Recovery to the unbent state was achieved by illuminating with visible light. These results show that here the effect of placing the azobenzene in the main chain oligomer does not only enhance the extent of the photoactuation at room temperature as previously reported,^[36] but it also reverses the bending direction. This bending motion away from the light was reversible for over 12 cycles of alternating UV and visible light with no signs of fatigue (Figure S5, Supporting Information).

LC actuators showing a directed motion away from the light source have been previously reported.^[24,37] In one case, fibers presenting side-chain azobenzene photoswitches bent away from the light source as a result of a free-volume generation from the *cis*-isomer at the illuminated surface.^[37] However, the current work employs the azobenzene as a crosslinker and this mechanism is therefore unlikely. In the other case, the uniaxial film that bent away from the light was the result of a photoinduced smectic (Sm) to nematic (N) transition that occurred at the illuminated surface.^[24] A similar mechanism could be

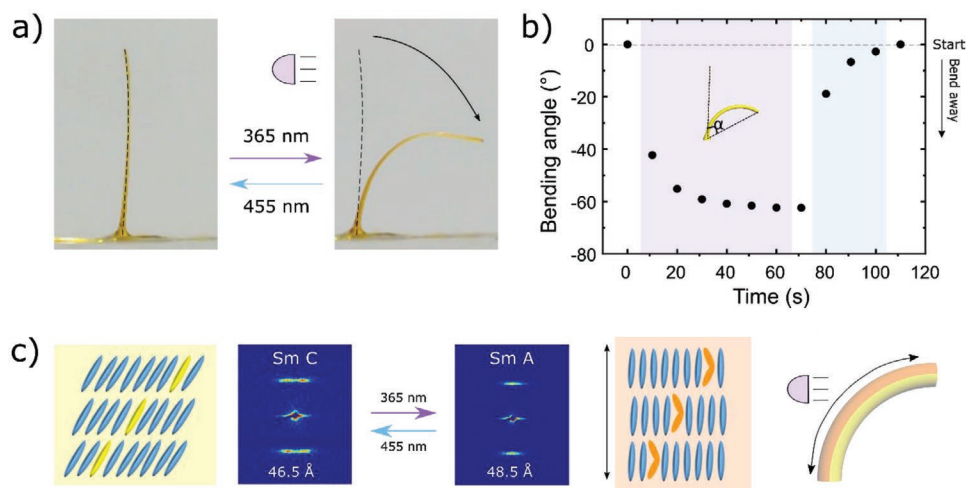


Figure 1. Photoactuation of a fiber. a) Side views of bending and unbending behaviors after irradiation with 365 and 455 nm lights. b) Bending angle as a function of irradiation time. Purple and blue regions indicate, respectively, the illumination with a 365 nm light and 455 nm light. The inset shows the definition of the bending angle used to characterize the motion of the standing fiber. c) 2D-SAXS patterns and interpreted mesogen alignment of fibers at room temperature after illumination with 365 and 455 nm light.

responsible for the hereto observed actuation directed away from the light source. Therefore, the mesogenic phase of a fiber under different illumination conditions was investigated by 2D small-angle X-ray scattering (2D-SAXS). As shown in Figure 1, in the small angle region, we observed a typical Sm C pattern with four small lobes before irradiation. Upon illumination with UV light, the four diffraction arcs integrated into two diffraction arcs, revealing the formation of a Sm A phase. After light irradiation, the average layer spacing increased from 46.5 Å with a tilt angle of 13° to 48.5 Å with no tilt. Furthermore, the Sm C to Sm A phase transition was not visible in the temperature-dependent 2D-SAXS measurements (Figure S6, Supporting Information), indicating that the phase transition was induced by the *cis*-azobenzene population formed by UV light illumination. We calculated the fractional layer spacing increase and the length increase at the illuminated surface (see Supporting Information). These calculations reveal that the bending away from the light motion is the result of the light-induced Sm C to Sm A phase transition, which is macroscopically manifested by an anisotropic expansion at the illuminated surface.

2.1.1. Direct Ink Writing of a Uniaxial Light-Responsive Polymer Film

The same LC-based ink was used for DIW to fabricate a uniaxial, light-responsive polymer film. The correlation between the alignment and the printing speed (2–13 mm s⁻¹) was investigated first (Figure S7, Supporting Information). The printing temperature was set to 40 °C and the nozzle diameter was 335 μm. Lines printed at speeds < 6 mm s⁻¹ displayed a non-variant brightness regardless of the orientation of the polarizer or analyzer, indicating different molecular orientations in the lines. Lines printed with speeds > 6 mm s⁻¹ were darker when parallel to the polarizer or analyzer than when at 45°. Such dark–bright states are associated with an orientated LCE along the axis of the printed line, that is, printing direction.^[30,31] This was further confirmed by a supplementary

optical characterization using the dichroism from the azobenzene (Figure S8, Supporting Information). From this data, the optimal printing speed was set to 13 mm s⁻¹.

With the optimized printing parameters, we printed a single-layer film (5 × 20 mm) on top of a glass substrate coated with polyvinylpyrrolidone (PVP) acting as sacrificial layer (Figure 2). After photopolymerization at room temperature, the LCE-film between crossed polarizers was darker when the longitudinal axis of the film was parallel to the polarizer or analyzer than when the axis was at 45° (Figure 2). This clearly indicated that the molecular orientation was achieved and successfully fixed, that is, a planar LCE-film was fabricated via DIW. Using a contact profiling system, we determined the thickness of the film to be on average 78 μm. After optical and structural characterization, the film was detached from the glass substrate by dissolving the PVP layer to obtain a free-standing film. Finally, the DSC traces of the film showed a $T_{I/N}$ around 82 °C, a significantly broad $T_{N/Sm}$ centered at 44 °C, and T_g at -25 °C, which is similar to the fibers (Figure S9, Supporting Information).

2.2. Stimuli-Response of the Printed LCE-Film

2.2.1. Characterization of the LCE-Film in Air

We first investigated the temperature-triggered response of the film using an oven. As previously reported for planar LCE-films,^[30,33] the film contracted along its long axis, parallel to the molecular director, and expanded perpendicular upon a temperature increase (Figure 2). When plotting the longitudinal shrinkage ratio (L/L_0) as a function of temperature, different stages of the response were observed (Figure 2). From 30 °C to ~40 °C, an increase of the film's length occurred due to the anisotropic thermal expansion. Then, a first actuation region was observed from ~40 °C until ~60 °C in which the film contracted because of the Sm C to N phase transition. A second actuation occurred from ~60 °C to ~80 °C, in which the film's length was

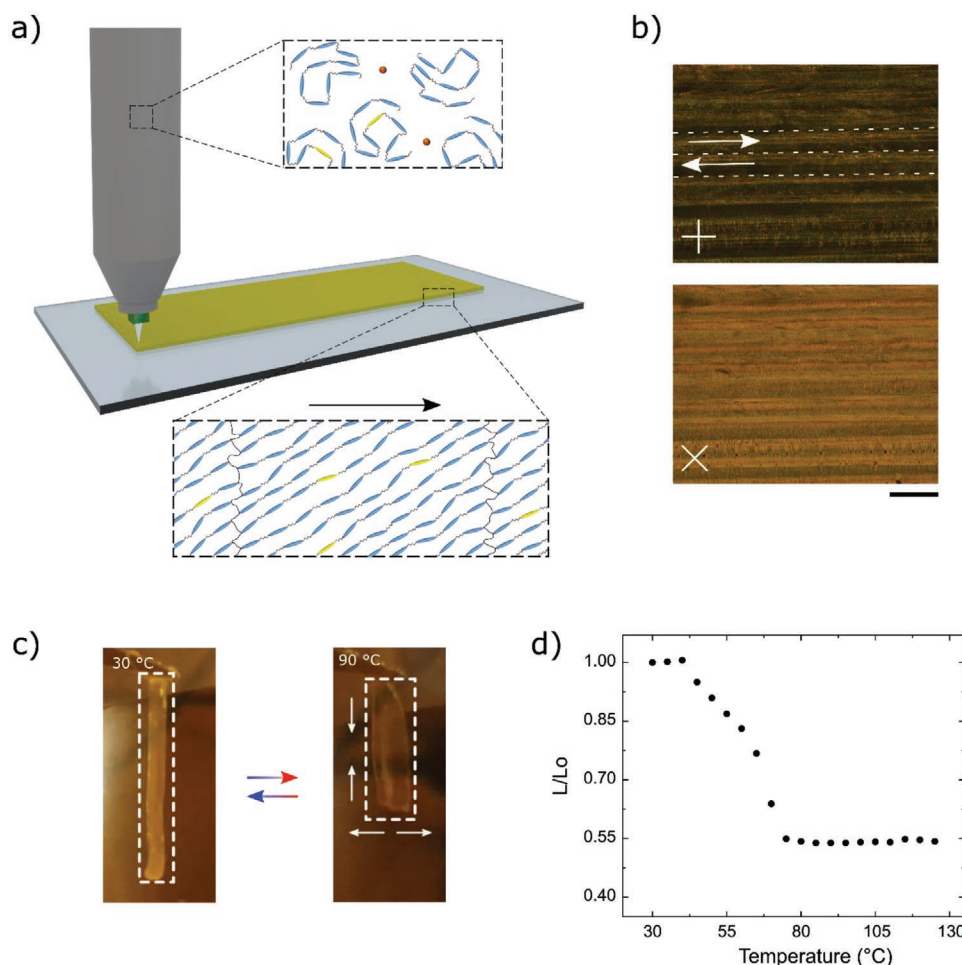


Figure 2. Overview of the fabrication and characterization of the printed LCE-film. a) Scheme of the printed set-up showing the alignment of the molecules at each stage. b) Polarized optical microscopy images of the printed film. The arrows indicate the printing direction and the dashed lines indicate the border of the lines that form the film. Scale bar represents 200 μm . c) Front images of the film at 30 °C and at 90 °C showing the anisotropic response of the film, contracting along its long axis and expanding along its width. d) Longitudinal shrinkage ratio (L/L_0) as a function of temperature. L represents the length of the film at a given temperature and L_0 the length at 30 °C.

further reduced due to the N to isotropic (I) phase transition. The second one being steeper due to the reduced temperature range at which the N to I transition occurs as seen in the DSC traces (Figure S9, Supporting Information). At ≈ 80 °C, the film was in its I phase and reached its maximum contraction, being around 50% of its initial length. From ≈ 80 °C to 125 °C a slightly positive length increase was observed due to the thermal expansion of the network. When cooling to 30 °C the film recovered its initial length (Figure S10, Supporting Information). The reversible temperature-dependent anisotropic contraction/expansion further confirms a homogeneous planar alignment through the thickness of the film.

To study the photoactuation, the printed LCE-film was clamped and hung on a stand as shown in Figure S11, Supporting Information. The film bent away from the light source as previously observed in the fibers (Figure 3; Movie S2, Supporting Information). Surprisingly, the response was obtained at lower light intensities; one order of magnitude smaller. We characterized the photoactuation by tracking the film's endpoint displacement under different light intensities and over

time (Figure 3). Increasing the light intensity increased the maximum bending angle until a plateau was reached. The maximum bending angle was attained after 5 min of 365 nm light (1.1 mW cm^{-2}) illumination. We recorded the film's surface temperature with a high-speed thermal camera (Figure S12, Supporting Information). No significant increase on temperature was observed during photoactuation, which indicates that the bending motion is mostly governed by photomechanical effects. When the light was turned off, the film remained in the bent state due to the long lifetime of the *cis*-azobenzene moieties at room temperature.^[22] Hence, different metastable bending angles could be obtained at different low light intensities (Figure S13, Supporting Information). Reversion to the initial shape, through 455 nm light (0.8 mW cm^{-2}) irradiation, took around 1 min. It is worth mentioning that when the film was exposed from the other side, it still bent away from the light source. The actuation rate of the film was slower than the photoactuation in the fiber. We speculate that the difference arises from the different geometries, objects sizes, and the lower light intensity used to actuate the film. Finally, the reversibility of

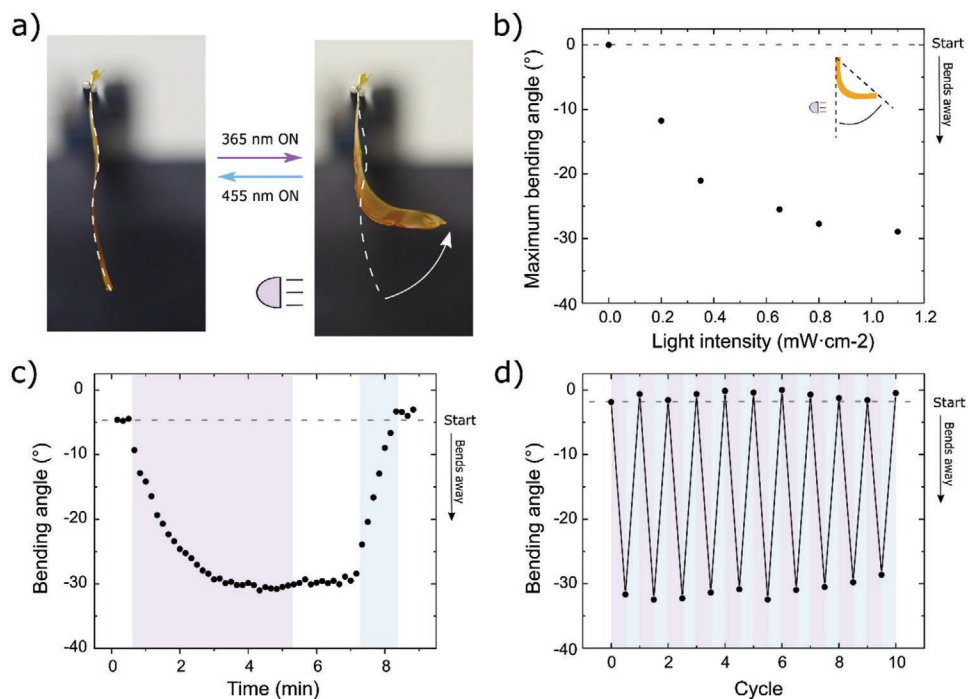


Figure 3. Photoactuation of the printed LCE-film in air. a) Edge-on images showing the bending motion from the light of the film upon 365 or 455 nm light irradiation from the left. b) Maximum bending angle obtained after 5 min of illumination with a 365 nm light at different intensities. The inset shows the definition of the bending angle used to characterize the motion of the film. c) Bending angle as a function of time when illuminated with a 365 and 455 nm light. d) Maximum bending angle of the film over ten successive cycles alternating illumination with 365 and 455 nm lights. For both (c) and (d), the purple and blue regions indicate, respectively, the illumination with a 365 nm light (1.1 mW cm⁻²) and 455 nm light (0.8 mW cm⁻²).

the photoactuation is demonstrated in Figure 3 in which after 10 cycles of alternating UV and visible light the film showed no signs of fatigue, similar to that previously observed for the fibers (Figure S5, Supporting Information). These results show that the printed LCE-film displays two different responses triggered by two distinct stimuli: light induces bending/unbending and temperature induces contraction/expansion.

2.2.2. Temperature-Dependent Photoactuation in Water

The underwater photoactuation was first studied by placing the hanging film in water at 20 °C, at which the polymer is in its Sm C phase (Figure 4; Figure S11, Supporting Information). Upon illumination with a 365 nm light (1.1 mW cm⁻²), the film bent away from the light source (Figure 4; Movie S3, Supporting Information). When the light was turned off, the film remained mostly bent, and slightly returned to its initial shape. Only when illuminated with 455 nm illumination (0.8 mW cm⁻²) did the film bend back to its initial state. The photoresponse in water at 20 °C showed a similar motion as in air while having a larger amplitude of actuation. If the thermal contribution to the back isomerization of the azobenzene moieties (*cis*→*trans*) is absent, as water acts as a heat sink, this might result in an overall higher *cis*-isomer population, hence in a larger actuation upon irradiation underwater in comparison with air.^[22,38,39] Drag forces in water were not observed to have a negative influence on the actuation amplitude.

Furthermore, we investigated the photoresponse of the polymer network in its N phase by heating the water to 60 °C.

Upon illumination with 365 nm light the film bent toward the light (Figure 4). After turning the light off, the film slowly returned to its initial state unlike in the experiment at 20 °C where the film remained stationary. In this case, the elevated temperature most likely reduces the lifetime of the *cis*-isomers. This reveals that it is difficult to keep the metastable state at higher temperature. Upon exposing the film to a 455 nm light, the film recovered faster to the unbent state. Figure S14 and Movie S4, Supporting Information, show a second actuation cycle at 60 °C in which a reduced time period between the illumination with 365 and 455 nm lights was used. In this second cycle, the photo-induced back isomerization is faster than the thermally induced one. In contrast to what occurs at room temperature (vide supra), at 60 °C the LCE-film is in its N phase and so isomerization of the azobenzene led to an increase of disorder in the network resulting in a contraction along the molecular axis and expansion perpendicular in the illuminated surface resulting in a bending motion toward the light motion.^[40] It should be noted that the temperature-dependent photoactuation was also observed for the drawn fibers showing that the atypical response is related to the light responsive ink (Figure S15, Supporting Information).

The temperature-dependent photoactuation of the film was further tracked by cooling the water from 60 to 20 °C while maintaining a constant UV light illumination (Figure 4). At 60 °C, the film bent toward the light source. While decreasing the temperature from 60 °C to ≈47 °C, the film maintained a constant deformation. Upon further cooling from ≈47 to 30 °C, the LCE network underwent a gradual phase transition from

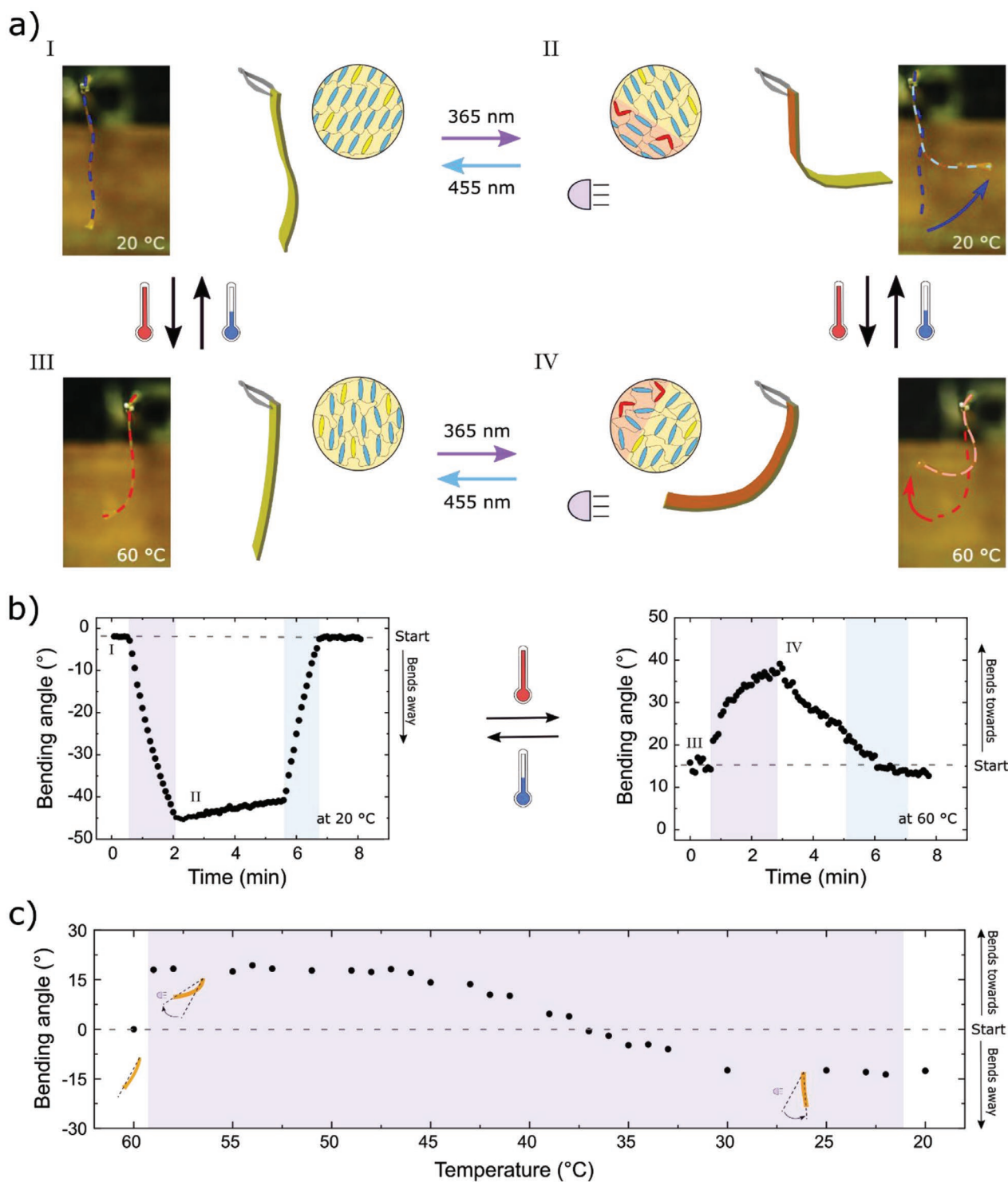


Figure 4. Temperature-dependent photoactuation of the printed LCE-film in water. a) Schematic representation and side-on images of the film during actuation as a response of two different stimuli: light and temperature. Temperature changes the LC phase of the film, from Sm C to nematic or vice versa. In the Sm C phase at low temperature, the film bends away from the light source. At high temperatures, in the nematic phase, the film bends toward the light source. Also, at elevated temperature the presence of convection flow, from right to left (as seen in Movie S4, Supporting Information), changes slightly the initial shape of the film. b) Bending angle as a function of irradiation time for a film at 20 °C (left) and 60 °C (right). The bending angle is defined in the inset in Figure 3. c) Photoactuation of the film in water at various temperatures while under continual 365 nm light exposure. In this case the starting position is set as the zero for the bent state, as shown in the left inset drawing. The other two schemes show the bend of the film at different temperatures with respect to the starting position. For both (b) and (c), the purple and blue regions indicate, respectively, the illumination with a 365 nm light (1.1 mW cm^{-2}) and 455 nm light (0.8 mW cm^{-2}).

N to Sm, resulting in an expansion along the long axis of the illuminated part of the film. Consequently, during this temperature range the film bent away from the light source. Below 30 °C, the film maintained a constant deformation, even when the light was turned off. As a result, the bending angle in the planar aligned film was reversed by decreasing the temperature from 60 to 20 °C. Recovery to the unbent state was achieved by illumination with 455 nm light at 20 °C (Figure S16, Supporting Information). These results show that different mechanisms govern the photoactuation of the LCE network at different temperatures and so the light-driven bending direction of the film can be controlled by tuning the temperature at which it is illuminated.

3. Conclusions

In conclusion, we have developed an LC oligomeric ink for the fabrication of amphibious light-fueled actuators via DIW. Remarkably, the light-triggered bending directionality can be regulated by temperature. When illuminated at room temperature, the LCE actuators undergo a light-induced phase transition from Sm C to Sm A that results in a motion directed away from the light source. Whereas when illuminated at elevated temperatures (>45 °C), the same actuator actuates toward the light source. These results show a new approach to control the photoinduced deformations in printed actuators and serve as an attractive method for the fabrication and design of light-fueled 3D actuators through additive manufacturing that operates both in air and underwater.

4. Experimental Section

Materials: 1,4-Bis-[4-(6-acryloyloxyhexyloxy) benzyloxy]-2-methylbenzene (**1**, RM82) was purchased from Merck. 4,4'-Bis(6-acryloyloxyhexyloxy) azobenzene (**2**, A6A) was purchased from Synthon. 3,6-Dioxa-1,8-octanedithiol (**3**, DODT) and 1,8-diazabicyclo[5.4.0]undec-7-ene (DBU) were obtained from Sigma-Aldrich. Base catalyst triethylamine (TEA) was obtained from Acros. Photoinitiator Irgacure 819, was purchased from Ciba. Polyvinylpyrrolidone with an average molecular weight of 40 000 g mol⁻¹ was purchased from Sigma-Aldrich. Solvent, dichloromethane (DCM) was obtained from Biosolve.

Characterization: ¹H NMR spectra were collected on a 400 MHz Bruker Advance III HD spectrometer with chloroform as solvent. GPC with was performed to evaluate the number average molecular weight (M_n), weight average molecular weight (M_w), and polydispersity index (PDI) of oligomers. Shimadzu apparatus was used for the GPC measurements using and the reference was polystyrene (PS) with an average M_w of 350 000 g mol⁻¹. DSC measurements were employed to determine the transition temperature of oligomers and fibers in a TA Instruments DSC Q1000. 2D-SAXS measurements were conducted on a Ganesha lab instrument with a GeniX-Cu ultralow divergence source producing X-ray photons equipped with a wavelength of 1.54 Å and a flux of 1×10^8 photons s⁻¹. A Pilatus 300 K silicon pixel detector with 478 × 619 pixels, each 172 μm² in size was utilized to collect scattering patterns. All microscopy images were taken from a Leica DM 2700M equipped with two polarizers that were operated either crossed or parallel, and a Linkam TMS 600 hot-stage. The thickness of the film was determined via a contact profile system, DektakXT from Bruker.

Preparation of the Ink: The oligomer was synthesized via a base-catalyzed thiol-acrylate Michael addition reaction. First, diacrylate

mesogen **1**, diacrylate azobenzene **2**, and dithiol chain extender **3** were added in a flask and dissolved in DCM. After mixing, TEA was slowly added to the solution. For large scale reactions, DBU was used instead of TEA (see Supporting Information). The feed ratios for each oligomer can be found in Table S1, Supporting Information. The mixture was reacted at 38 °C overnight. Then, DCM was added to the flask to dilute the mixture and washed with 1 M HCl (2×) and saturated brine (1×) to remove the existing TEA. The organic phase was collected and dried with MgSO₄. Subsequently, most of solvent was removed by a rotary evaporator in filtrate. The removal of the residual solvent was conducted in a vacuum oven at room temperature. Finally, the oligomer (98 wt%) was mixed with the photoinitiator (2 wt%) in DCM. The ink was obtained after removing the solvent at room temperature under vacuum.

Fabrication of Standing Fibers: In general, the fibers were fabricated via a drop casting/drawing technique as previously reported.^[23] The ink was dissolved in DCM (270 mg mL⁻¹) at room temperature. Droplets with 10 μL solution were cast on a glass substrate (3 × 3 cm²) and heated at 60 °C for 30 min to remove the solvent. After that, the substrate supporting the droplets was gently contacted by another glass plate from above. Fibers were obtained from the viscous droplets after two glass plates were pulled apart 1.25 cm. The randomly oriented mesogens were uniaxially aligned along the longitudinal direction due to the elongational flow of the drawing process. The homogeneously oriented mesogens were subsequently photocrosslinked under nitrogen atmosphere with an Exfo Omnicure S2000 light source in which 57% of the light intensity has a wavelength of 395–445 nm and 43% of 320–390 nm. A light filter was utilized to block wavelengths below 405 nm, limiting the formation of *cis*-isomerized azobenzene. After photocrosslinking for 1 h, standing fibers on the glass substrate were achieved after cutting the fiber tops with a scissor and removing the top glass plate.

Direct Ink Writing: The printing process was performed using a commercial 3D printer (EHR, Hyrel 3D). The ink was loaded into the stainless-steel reservoir at room temperature and extruded using a nozzle diameter of 335 μm at 40 °C. The printing speed ranged between 2–13 mm s⁻¹, being 13 mm s⁻¹ the optimal one. A film (5 × 20 mm²) was printed on top of a PVP-coated glass. The printing path was controlled by a G-code generated by the printer software. After printing, photopolymerization was induced using an Exfo Omnicure S2000 light source in which 57% of the light intensity has a wavelength of 395–445 nm and 43% of 320–390 nm. A light filter was utilized to block wavelengths below 405 nm, limiting the formation of *cis*-isomerized azobenzene. After exposure for 2 h, in which the sample was flipped every 30 min, the film's thickness and birefringence was characterized via a profiling system and a microscope, respectively. To obtain a free-standing film, the PVP layer was dissolved by immersing the sample in water at room temperature and subsequently dried at room temperature overnight.

Photoactuation of the Fibers and the Film: Fibers and film, either standing or hanging, were placed at 21.0 cm distance from collimated UV light (365 nm, Thorlabs M365L2) and visible light (455 nm, Thorlabs M455L3-C2). A controller (ThorLabs DC4104) was used to tune the intensity of the lights. All objects were illuminated with the 455 nm light before performing the photoactuation to ensure that all azobenzene molecules were in the *trans*-isomer. A camera (Nikon D7200, Olympus OM-D E-M10 Mk III) was used to record the light-driven deformation. The temperature of the surface of the film was controlled using a Gobi camera from Xenics. Underwater actuation was conducted inside a transparent container with flat sides that was filled with water either at 20 °C or at 60 °C (Figure S11, Supporting Information). The temperature of the water was controlled using a digital thermometer.

Supporting Information

Supporting Information is available from the Wiley Online Library or from the author.

Acknowledgements

M.d.P. and L.L. contributed equally to this work. M.d.P. acknowledges the funding from the Netherlands Organization for Scientific Research (NWO) in the framework of Innovation Fund Chemistry and Dutch Ministry of Economic Affairs in the framework of the PPP allowance. L.L. would like to acknowledge the financial support from China Scholarship Council (CSC). D. C. Hoekstra is acknowledged for GPC measurements. R. C. P. Verpaalen is acknowledged for 2D-SAXS measurements. M. G. Debije and J. A. H. P. Sol are acknowledged for useful discussion regarding the manuscript and DIW work, respectively.

Conflict of Interest

The authors declare no conflict of interest.

Keywords

4D printing, amphibious, direct ink writing, light-responsive polymers, liquid crystal actuators

Received: July 2, 2020

Revised: August 4, 2020

Published online: September 13, 2020

- [1] B. Xu, C. Zhu, L. Qin, J. Wei, Y. Yu, *Small* **2019**, *15*, 1901847.
- [2] A. Kotikian, C. McMahan, E. C. Davidson, J. M. Muhammad, R. D. Weeks, C. Daraio, J. A. Lewis, *Sci. Rob.* **2019**, *4*, eaax7044.
- [3] J. A. H. P. Sol, A. R. Peeketi, N. Vyas, A. P. H. J. Schenning, R. K. Annabattula, M. G. Debije, *Chem. Commun.* **2019**, *55*, 1726.
- [4] L. Yu, H. Shahsavan, G. Rivers, C. Zhang, P. Si, B. Zhao, *Adv. Funct. Mater.* **2018**, *28*, 1802809.
- [5] T. H. Ware, T. J. White, *Polym. Chem.* **2015**, *6*, 4835.
- [6] R. C. P. Verpaalen, M. G. Debije, C. W. M. Bastiaansen, H. Halilović, T. A. P. Engels, A. P. H. J. Schenning, *J. Mater. Chem. A* **2018**, *6*, 17724.
- [7] L. T. De Haan, J. M. N. Verjans, D. J. Broer, C. W. M. Bastiaansen, A. P. H. J. Schenning, *J. Am. Chem. Soc.* **2014**, *136*, 10585.
- [8] A. H. Gelebart, D. J. Mulder, M. Varga, A. Konya, G. Vantomme, E. W. Meijer, R. L. B. Selinger, D. J. Broer, *Nature* **2017**, *546*, 632.
- [9] R. C. P. Verpaalen, S. Varghese, A. Froyen, M. Pilz da Cunha, M. J. Pouderoijen, J. R. Severn, M. R. Bhatti, T. Peijs, C. W. M. Bastiaansen, M. G. Debije, T. A. P. Engels, A. P. H. J. Schenning, *Matter* **2020**, *2*, 1522.
- [10] E. C. Davidson, A. Kotikian, S. Li, J. Aizenberg, J. A. Lewis, *Adv. Mater.* **2020**, *32*, 1905682.
- [11] A. H. Gelebart, D. J. Mulder, G. Vantomme, A. P. H. J. Schenning, D. J. Broer, *Angew. Chem., Int. Ed.* **2017**, *56*, 13436.
- [12] P. Zhu, W. Yang, R. Wang, S. Gao, B. Li, Q. Li, *ACS Appl. Mater. Interfaces* **2018**, *10*, 36435.
- [13] J. Thévenot, H. Oliveira, O. Sandre, S. Lecommandoux, *Chem. Soc. Rev.* **2013**, *42*, 7099.
- [14] H. K. Bisoyi, Q. Li, *Chem. Rev.* **2016**, *116*, 15089.
- [15] M. Pilz da Cunha, S. Ambergen, M. G. Debije, E. F. G. A. Homburg, J. M. J. den Toonder, A. P. H. J. Schenning, *Adv. Sci.* **2020**, *7*, 1902842.
- [16] T. J. White, *J. Polym. Sci., Part B: Polym. Phys.* **2018**, *56*, 695.
- [17] H. Yu, T. Ikeda, *Adv. Mater.* **2011**, *23*, 2149.
- [18] M. Pilz da Cunha, Y. Foelen, R. J. H. van Raak, J. N. Murphy, T. A. P. Engels, M. G. Debije, A. P. H. J. Schenning, *Adv. Opt. Mater.* **2019**, *7*, 1801643.
- [19] O. M. Wani, R. Verpaalen, H. Zeng, A. Priimagi, A. P. H. J. Schenning, *Adv. Mater.* **2019**, *31*, 1805985.
- [20] O. M. Wani, H. Zeng, A. Priimagi, *Nat. Commun.* **2017**, *8*, 15546.
- [21] H. Shahsavan, A. Aghakhani, H. Zeng, Y. Guo, Z. S. Davidson, A. Priimagi, M. Sitti, *Proc. Natl. Acad. Sci. U. S. A.* **2020**, *117*, 5125.
- [22] M. Pilz da Cunha, E. A. J. van Thoor, M. G. Debije, D. J. Broer, A. P. H. J. Schenning, *J. Mater. Chem. C* **2019**, *7*, 13502.
- [23] A. H. Gelebart, M. Mc Bride, A. P. H. J. Schenning, C. N. Bowman, D. J. Broer, *Adv. Funct. Mater.* **2016**, *26*, 5322.
- [24] Y. Zhang, J. Xu, F. Cheng, R. Yin, C. C. Yen, Y. Yu, *J. Mater. Chem.* **2010**, *20*, 7123.
- [25] R. L. Truby, J. A. Lewis, *Nature* **2016**, *540*, 371.
- [26] T. D. Ngo, A. Kashani, G. Imbalzano, K. T. Q. Nguyen, D. Hui, *Composites, Part B* **2018**, *143*, 172.
- [27] M. O. Saed, C. P. Ambulo, H. Kim, R. De, V. Raval, K. Searles, D. A. Siddiqui, J. M. O. Cue, M. C. Stefan, M. R. Shankar, T. H. Ware, *Adv. Funct. Mater.* **2019**, *29*, 1806412.
- [28] D. J. Roach, X. Kuang, C. Yuan, K. Chen, H. J. Qi, *Smart Mater. Struct.* **2018**, *27*, 125011.
- [29] Y. Zhang, L. Huang, H. Song, C. Ni, J. Wu, Q. Zhao, T. Xie, *ACS Appl. Mater. Interfaces* **2019**, *11*, 32408.
- [30] M. López-Valdeolivas, D. Liu, D. J. Broer, C. Sánchez-Somolinos, *Macromol. Rapid Commun.* **2018**, *39*, 1700710.
- [31] C. P. Ambulo, J. J. Burroughs, J. M. Boothby, H. Kim, M. R. Shankar, T. H. Ware, *ACS Appl. Mater. Interfaces* **2017**, *9*, 37332.
- [32] G.-Z. Yang, R. J. Full, N. Jacobstein, P. Fischer, J. Bellingham, H. Choset, H. Christensen, P. Dario, B. J. Nelson, R. Taylor, *Sci. Rob.* **2019**, *4*, eaaw1826.
- [33] A. Kotikian, R. L. Truby, J. W. Boley, T. J. White, J. A. Lewis, *Adv. Mater.* **2018**, *30*, 1706164.
- [34] C. Zhang, X. Lu, G. Fei, Z. Wang, H. Xia, Y. Zhao, *ACS Appl. Mater. Interfaces* **2019**, *11*, 44774.
- [35] J. del Barrio, C. Sánchez-Somolinos, *Adv. Opt. Mater.* **2019**, *7*, 1900598.
- [36] L. Liu, M. Pozo, F. Mohseninejad, M. G. Debije, D. J. Broer, A. P. H. J. Schenning, *Adv. Opt. Mater.* **2020**, 2000732.
- [37] Z. Cheng, S. Ma, Y. Zhang, S. Huang, Y. Chen, H. Yu, *Macromolecules* **2017**, *50*, 8317.
- [38] M. Pilz da Cunha, H. S. Kandail, J. M. J. den Toonder, A. P. H. J. Schenning, *Proc. Natl. Acad. Sci. U. S. A.* **2020**, *117*, 17571.
- [39] R. C. P. Verpaalen, M. Pilz da Cunha, T. A. P. Engels, M. G. Debije, A. P. H. J. Schenning, *Angew. Chem., Int. Ed.* **2020**, *59*, 4532.
- [40] C. L. van Oosten, K. D. Harris, C. W. M. Bastiaansen, D. J. Broer, *Eur. Phys. J. E: Soft Matter Bio. Phys.* **2007**, *23*, 329.